

Experimental and numerical study on the crashworthiness evaluation of an intercity coach under frontal impact conditions

Mehmet Ali Güler^{1,2} , Muhammed Emin Cerit³,
Sinem Kocaoglan Mert⁴ and Erdem Acar²

Proc IMechE Part D:
J Automobile Engineering
2020, Vol. 234(13) 3026–3041
© IMechE 2020
Article reuse guidelines:
sagepub.com/journals-permissions
DOI: 10.1177/0954407020927644
journals.sagepub.com/home/pid


Abstract

In this study, the energy absorption capacity of a front body of a bus during a frontal crash was investigated. The strength of the bus structure was examined by considering the ECE-R29 European regulation requirements. The nonlinear explicit finite element code LS-DYNA was used for the crash analyses. First, the baseline bus structures without any improvements were analyzed and the weak parts of the front end structure of the bus body were examined. Experimental tests are conducted to validate the finite element model. In the second stage, the bus structure was redesigned in order to strengthen the frontal body. Finally, the redesigned bus structure was compared with the baseline model to meet the requirements for ECE-R29. In addition to the redesign performed on the body, energy absorption capacity was increased by additional energy absorbers employed in the front of bus structure. This study experimentally and numerically investigated the energy absorption characteristics of a steering wheel armature in contact with a deformable mannequin during a crash. Variations in the location of impact on the armature, armature orientation, and mannequin were investigated to determine the effects of the energy absorption characteristics of the two contacting entities.

Keywords

Crashworthiness, frontal crash, explicit dynamics, ECE R-29, LS-DYNA

Date received: 2 December 2019; accepted: 3 April 2020

Introduction

The understanding and exploration of the energy absorption capacity of automotive components is vital for the development of safe and durable vehicles. Today's indispensable transportation vehicles, including automobiles and buses, are mostly used when traveling long distances. For various reasons, traffic accidents can occur between two vehicles, or between a vehicle and pedestrian. Although precautions are taken to prevent such accidents, they are inevitable. Owing to the weight and speed of a bus during crash, the crash energy is very high and directly affects the driver and passengers. Buses needed to be designed to decrease the risk of injury to the occupants. Better crashworthiness of the bus minimizes the effect of crash to the occupants.

Investigations on accidents involving busses or coaches showed that the majority of these accidents are either frontal crash, rollover, side and rear crash, or a combination of these. The Enhanced Coach and Bus Occupant Safety (ECBOS) project was involved in investigating the accidents that occurred in eight

European countries (Austria, France, Germany, United Kingdom, Italy, Netherlands, Spain, and Switzerland). They concluded that in some countries, the frontal crash reaches up to 70% among all types of bus accidents. In the bus occupant safety report, it is reported that riding in a coach or bus is 10 times safer than riding in other transportation vehicles.¹

¹College of Engineering and Technology, American University of the Middle East, Kuwait

²Department of Mechanical Engineering, TOBB University of Economics and Technology, Ankara, Turkey

³The Scientific and Technological Research Council of Turkey—Defense Industries Research and Development Institute (TÜBİTAK SAGE), Ankara, Turkey

⁴Department of Mechanical Engineering, Ankara Yıldırım Beyazıt University, Ankara, Turkey

Corresponding author:

Mehmet Ali Güler, College of Engineering and Technology, American University of the Middle East, Kuwait.

Emails: mehmet.guler@aum.edu.kw; mguler@etu.edu.tr;

prof.guler@gmail.com

A similar statistical study conducted by Transport Canada in U.S. provided a detailed report on the accidents in Canada, United States, and Europe. According to this report, a total of 20,000 accidents occur annually, and bus accidents constitute 4% of the total accidents. In addition, more than 35,000 people get injured in accidents involving busses.²

According to a recent study by the National Highway Traffic Safety Administration (NHTSA), a department of the US Department of Transportation, 41% of the accidents occurring in United States were found to be frontal crash accidents. This ratio shows the importance of studying the frontal crash among other types of accidents for driver safety.³

In case of a frontal crash, the drivers and couriers are at a great risk. Huge crash energies can occur when a bus hits a truck or another bus (e.g. a bus weighing 13 tons and traveling at 50 km/h). In case of a frontal crash, most of the crash energy is directly absorbed by the front body structure, and ultimately the survival space of the driver and courier will be intruded by the plastic deformation of the structure.

Some studies analyzed the frontal crashworthiness of buses or trucks including regulations for their safety. Raich and DaimlerChrysler⁴ investigated the frontal crash behavior of a truck according to the ECE Regulation 29 by performing numerical analysis and tests. He remodeled the truck cabin and pedal box to prevent an intrusion to the survival space of the driver.

Matolcsy⁵ designed a safety bumper system by using crush boxes in the front body structure of a bus. Rectangular steel tubes (40 mm × 40 mm × 2 mm) and several tube combinations (e.g. single, double, triple, and quadruple) were used in the crushbox design to minimize the peak force and absorb maximum energy. They tried to control the buckling behavior by investigating the deformation behavior during a crash.

Marzbanrad et al.⁶ investigated geometry and impact condition of a front bumper beam made of aluminum, glass mat thermoplastic (GMT) and high-strength sheet molding compound (SMC) to under low-velocity impact. Impact is simulated according to ECE. United Nations Agreement, Regulation no. 42, 1994. The results showed that deflection, impact force and stress distribution can be decreased and the elastic strain energy can be increased with SMC bumper beam.

Tech et al.⁷ modeled the whole bus structure and studied the frontal impact of a bus against a rigid wall. They applied 48 km/h as the impact velocity to be consistent with the United States FMVSS/208 passenger protection against frontal vehicle crash (NHTSA, fmvss/208 status report for frontal offset crash testing). They also performed impact tests on 1.5 long bars, conducted finite element analysis (FEA) and validated their FEA model through experiments.

De Coe et al.⁸ studied the safety of drivers and couriers of coaches in frontal crashes. They investigated the scenario of a bus colliding with the rear end of a truck.

They added a crushbox composed of several tubular structures and an air vessel as the crash energy absorber.

Griškevičius and Žiliukas⁹ conducted a study investigating the ability of vehicles to absorb energy in frontal crashes. In the study, four characteristic materials were used on the main beam with two cross-sectional shapes. LS-DYNA models were prepared, in which the front parts of the vehicle, such as column, bottom frame, and tunnel were fixed while the main beams were variable. These models were simulated according to the EURO-NCAP (the vehicle hits a deformable barrier with 40% offset at 64 km/h) and United States-New Car Assessment Program (US-NCAP; the vehicle hits a rigid barrier with 100% of its front at 56 km/h). The analysis according to both standards showed that the main beam, to which the tampon was connected, was the most exposed front part element.

Öztürk and Kaya¹⁰ studied the impact absorption characteristics of the front bumper system of a car exposed to a 40% offset crash. DP600 high strength steel was chosen for the design of the buffer system. After the approximate design geometry was created, an optimization was performed in MATLAB, and the optimum sheet thickness was determined as 1 mm. The LS-DYNA model was created to simulate a crash with 40% offset of the bumper beam and energy absorbers. The crash simulation was modeled as a rigid block of 1000 kg, with an offset of 40% at 57 km/h. Simulations have shown that the number of buckling initiator zones does not cause a significant change in the total energy absorbed but reduces the maximum reaction force.

Kokkula et al.¹¹ conducted a study to increase sensitivity in the numerical modeling of bumper beam-longitudinal systems and obtain more accurate results. Numerical simulations were performed on bumper beam-longitudinal systems subjected to 40% offset impact carried out using the non-linear finite element code LS-DYNA and compared with experimental results. A detailed mathematical modeling of the system was obtained through the detailed modeling of the part production and connection methods.

The studies on the crashworthiness and safety assessment of the buses are limited compared to the studies related to bumper systems and crash boxes. Study of Kwasniewski et al.¹² describe an assessment for the crashworthiness and safety assessment of paratransit buses in the state of Florida. Worldwide vehicle safety standards were adopted in the study with modifications addressing the bus construction process and relevance of particular structural components in crash events. Passenger compartment, which needs to be protected against side impact and rollover, is a major area of concern in the standard. Therefore, this study presents the results of the computer simulations for the rollover and the side impact tests.

Güler et al.¹³ studied ECE-R66 rollover crash analyses of a stainless-steel bus and the strength of the vehicle is assessed according to the requirements of the

regulation. Starting from a baseline design, different models and worst case assumptions were investigated. The results indicated that belted passengers increase the energy 37% during rollover.

Güler et al.¹⁴ evaluated the structural resistance and passenger injury risks and compared the effectiveness of safety belt usage during a rollover event. In that study, a total of eight occupants were placed in the structurally weakest sections of the 13-m-long TEMSA bus. Three occupant protection cases; no safety belt, two-point safety belt, and three-point safety belt were investigated. A standard rollover procedure was simulated using non-linear finite element code LS-DYNA. According to the simulation results; if there was no seat belt protection, occupants suffered serious risk of injuries. Also, similar protection levels observed for two- and three-point safety belts.

Demirci and Yıldız¹⁵ investigated the crash performances of SPC 440 and DP-TRIP steels, AA7108—AA7003 aluminum alloys, AM60—AZ31 magnesium alloys and thin-walled tube cross-sections numerically to obtain light-weight vehicle design. According to their study, the total energy absorption and the specific energy absorption (SEA) of circular and polygonal tubes were better than square and rectangular tubes for both straight and tapered models independent of material. However, the peak crush forces of circular and polygonal tubes were found to be higher than square and rectangular tubes for all models.

Tanlak et al.¹⁶ performed a geometrical optimization for the box-shaped bumper beams. The crash phenomenon was simulated in standard tests, in which the vehicle hit a deformable barrier with an offset of 40% at 64 km/h. In that study, two optimum shapes showed significant improvement over the current shape, and the optimal beam absorbed 16% larger specific strain energy. At low speeds, the resistance to crash was improved.

Xiao et al.¹⁷ studied a bumper beam filled with functionally graded foam (FGF) under both frontal and offset impact. The effects of foam density grading, foam density range and wall thickness on the crashworthiness were investigated. The Kriging surrogate modeling and multiobjective particle swarm optimization (MOPSO) algorithm were used to seek an optimum design by considering SEA, and peak force as the design objectives. They found that the use of FGF-filled bumper beam reduced the beam weight about 14.4% compared to baseline bumper beam without losing crashworthiness performance of the car.

Belingardi et al.¹⁸ investigated pultruded composite car bumper beam to improve mechanical properties and energy absorption capability while reducing weight. They compared E-Glass/epoxy pultruded bumper beam and its energy absorption capability with steel and E-Glass/epoxy fabric composite. They simulated low-velocity impact using ABAQUS to optimize bumper beam section profile and beam curvature. They found

that pultruded bumper beam improved energy absorption characteristics and had lower mean crash load.

Optimization algorithms to improve crashworthiness of a vehicle were studied by Kiani and Yıldız¹⁹ along with Karagöz and Yıldız.²⁰ Kiani and Yıldız¹⁹ analyzed peak acceleration and internal energy under frontal, offset, and side crash. A nonlinear surrogate-based mass minimization was conducted by applying radial basis functions surrogate models. The differential evolution algorithm was found best optimization method among artificial bee colony, genetic algorithm, particle swarm, and simulated annealing algorithms.

Karagöz and Yıldız²⁰ aimed to find optimum thin-walled tube with minimum weight and maximum energy absorption performance considering effect of the forming history. The performances of particle swarm algorithm, cuckoo search algorithm, gravitational search algorithm (GSA), hybrid gravitational search-Nelder Mead algorithm (HGSANM), league championship algorithm (LCA), firefly algorithm, bat algorithm, interior search algorithm (ISA) and imperialist competitive algorithm (ICA) were studied to obtain the optimum tube. The hybrid GSA was found the most successful algorithm among the nine optimization algorithms. Due to the forming process, a significant effect on energy absorption of thin-walled tubes was observed.

The main purpose of this study was to determine the weak parts of the front-end structure of the bus body and strengthen the frontal body. To simulate the crash behavior of the bus, and explicit dynamic FEA code LS-DYNA was used. In this study, the energy absorption behavior of a steering wheel armature in contact with a deformable chestform (bodyform) during a crash was experimentally and numerically investigated. To improve the energy absorption of the bus, an improved energy absorber was constructed in the reinforced body. The energy absorption characteristics of the energy absorbers were analyzed independently of the bus body, and detailed results were obtained.

The paper is structured as follows. Section 'Introduction' introduces the test standards for heavy vehicles. Section 'Test standard for heavy vehicles' describes the finite element model and the experimental setup used in validation study is given in section 'Finite element model'. Section 'Experimental setup and validation' presents the numerical results. Finally, section 'Numerical results' lists the conclusions drawn from this study.

Test standard for heavy vehicles

The condition for frontal crash accident is standardized for heavy vehicles by the United Nations Economic Commission for Europe (UNECE). ECE R29 regulation, which has become compulsory by UNECE, involves roof and rear-wall strengthening tests besides front impact test.²¹

For the frontal crash test, a pendulum plate with a mass, width, and height of 1500 ± 250 kg, 2500 mm and 800 mm respectively, and made of steel was used. The length of the arms connecting the pendulum plate to the pendulum test setup must be at least 3500 mm from the center of gravity of the pendulum plate. The required crash energy to be given to the vehicle during the test varies depending on the vehicle tonnage. While a kinetic energy of 30 kJ is required for the vehicles with a weight of less than 7 tons, the crash energy is specified at ECE R29 regulation as 45 kJ for vehicles of more than 7 tons. As the total weight of the vehicle used in this study is more than 7 tons, the crash energy was 45 kJ.

The connection of the vehicle to the test setup is specified in ECE R29. The vehicle is not attached to the ground rigidly but positioned on wooden blocks. The vehicle chassis is positioned on the wooden blocks and attached to the ground with steel chains. These chain connections are shown in Figures 1 and 2.

To determine whether the frontal crash test meets the ECE R29 regulatory requirements, a foam material driver model was used. Figure 3 shows the 50th percentile male mannequin, as described in ECE R29 regulation. For the test to be successful, none of the parts must encroach into the survival space of the driver during the frontal impact test.

Finite element model

The finite element model of the bus body structure was constructed using ANSA,²² and the crash analyses were performed through an explicit nonlinear finite element code LS-DYNA.²³ A crash analysis was performed using a pendulum weighing 1500 kg in accordance with the criteria specified in ECE R29 regulation. The constructed finite element model consists of the structure of the front body of a bus, front chassis, lower chassis, side walls, roof, steering system, and driver seat. The computer-aided design (CAD) model of the bus body was constructed through CATIA²⁴ and the finite element mesh was constructed using ANSA.²² The finite

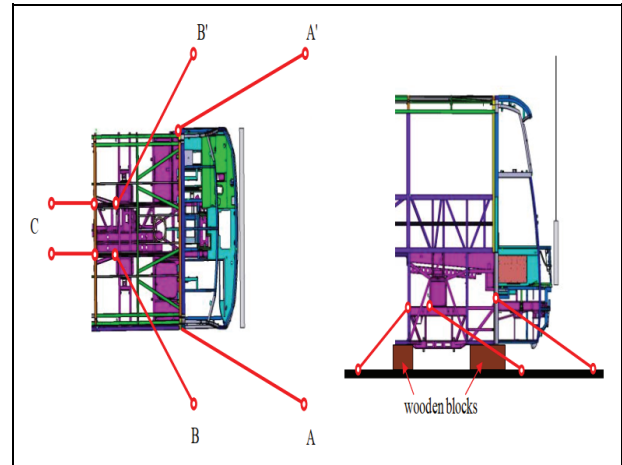


Figure 1. Anchoring chain connections according to ECE R29.

element model of the bus structure shown in Figure 4 consists of 550,076 nodes and 544,378 shell elements with 442,451 and 101,927 deformable and rigid elements, respectively. The boundary conditions of the FEA model are given in Figure 5. The bus body structure was ideally fixed in six degrees of freedom (DOFs) to the ground from the frames which belong to the lower chassis (see Figure 2). This idealized boundary condition is assumed to have ignorable effects in terms of the FEA results since the fixed boundary region is sufficiently far away from the region of interest which is the front chassis and the driver compartment. The effects of the chains are ignored.

While the general size for the shell elements was selected to be $10\text{ mm} \times 10\text{ mm}$, this value was decreased to $2\text{ mm} \times 2\text{ mm}$ for the critical regions requiring more attention. The front regions of the bus structure, and especially the energy absorbers, were modeled using a finer mesh structure. The Belytschko-Lin-Tsay shell elements with five integration points through the thickness were employed in the FEA modeling. The Belytschko-Lin-Tsay shell elements were used because of their cost efficiency, which is desirable in mathematical operations.²³

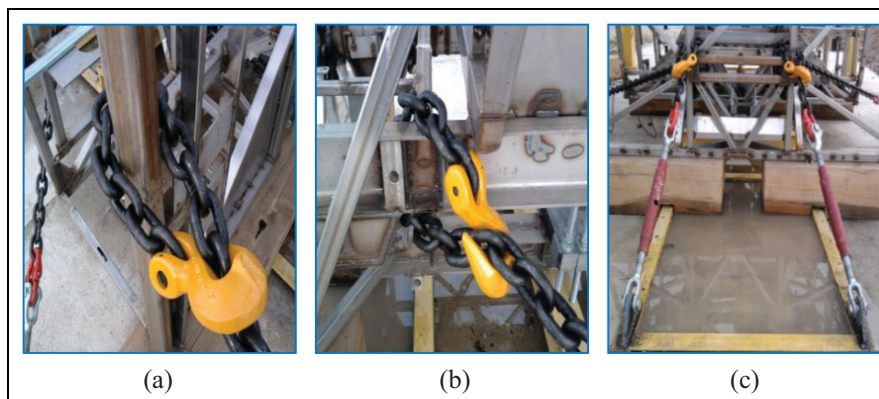


Figure 2. Chain connections in different views (a) upper, (b) frontal, and (c) distant.

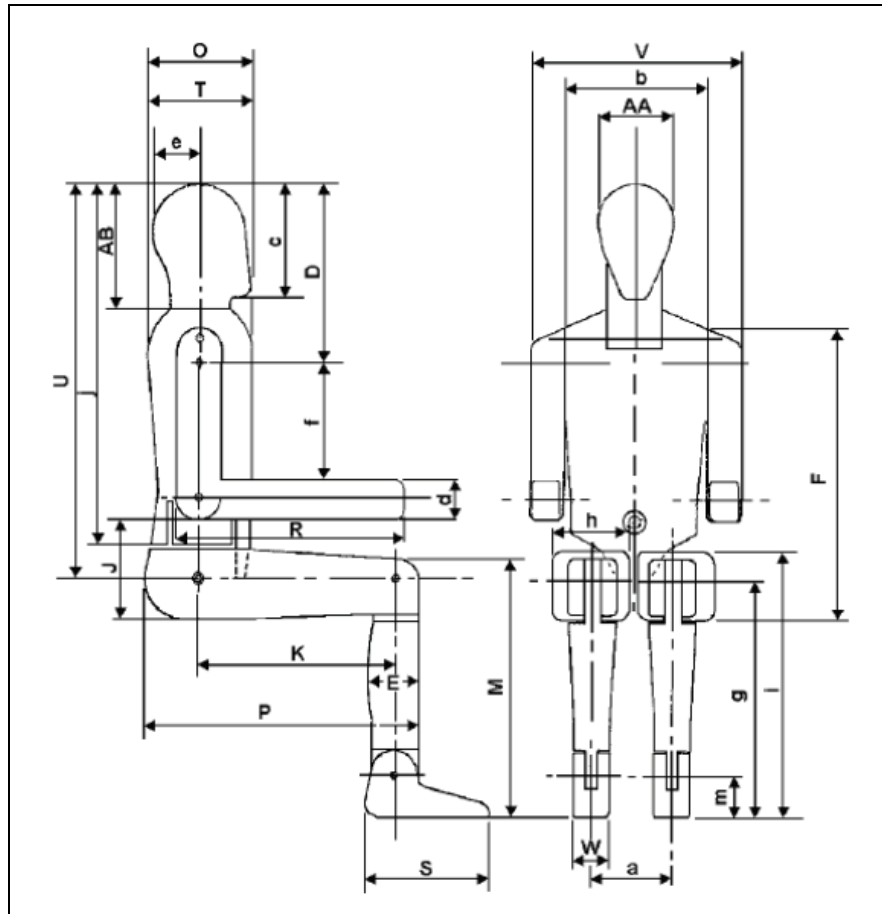


Figure 3. Fiftieth-percentile male mannequin used to verify the survival space.²¹

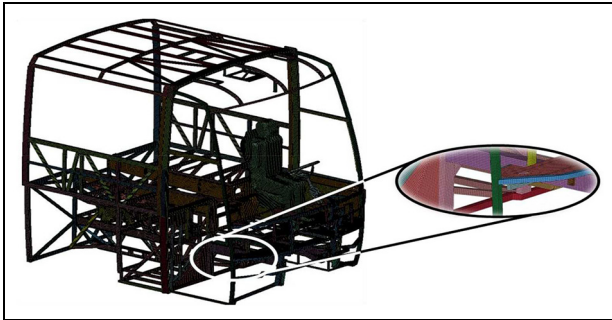


Figure 4. Finite element mesh of the bus structure.

Different material definitions were used for the bus body structure and pendulum geometry. While the material definition of *MAT RIGID (Type 20) was used for the rigid pendulum plate, *MAT PIECEWISE LINEAR PLASTICITY (Type 24) and *MODIFIED MAT PIECEWISE LINEAR PLASTICITY (Type 123) material models were used for the deformable parts constituting the bus body structure. Material model Types 24 and 123 were used as the elasto-plastic material models in which elastic and plastic regions of the stress-strain curve can be included with true stress-true plastic strain curves. In material model Type 123, the failure strain can be defined as distinct from

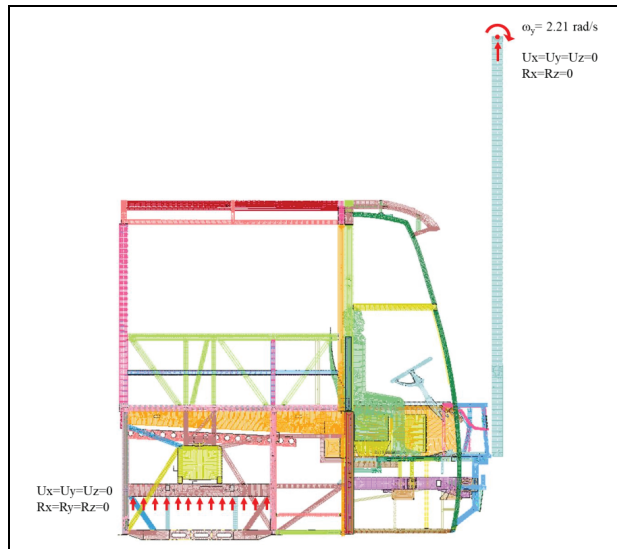


Figure 5. Boundary conditions applied to the FEA model of the bus structure.

material model Type 24. Therefore, more realistic material failure for shell elements can be defined. The material used for the bus body structure was DIN 1.4003 stainless steel.

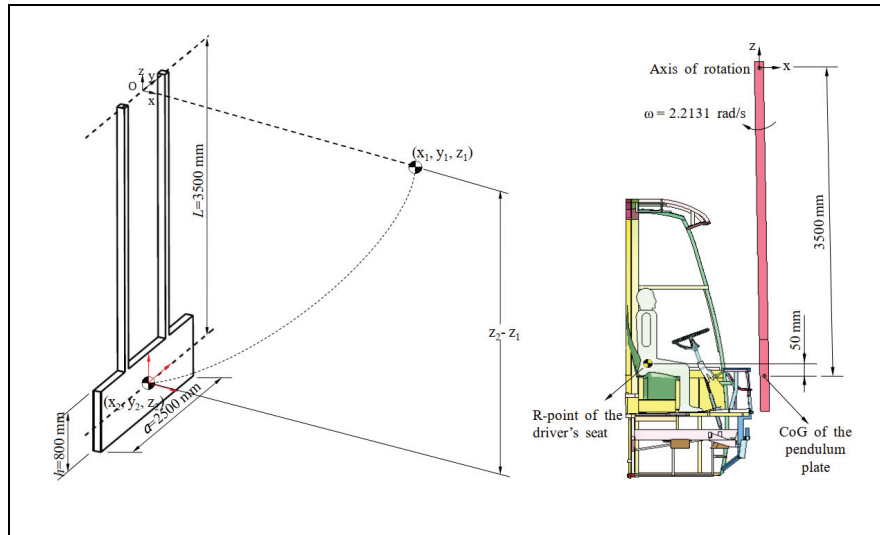


Figure 6. Dimensions of the pendulum plate and position with respect to R-point.

The contact definition of the parts constituting the bus body and self-contact of the parts was defined through *CONTACT AUTOMATIC SINGLE SURFACE. Automatic contact definitions are usually used when the deformations occur rapidly, especially in crash analyses. Furthermore, the contact definition of *CONTACT AUTOMATIC SURFACE TO SURFACE was used to define the contact between the bus body and rigid pendulum. The static and dynamic friction coefficients were specified as 0.3 and 0.2 for the contact definitions, respectively.

In order for the pendulum to satisfy the required crash energy, its mass, mass moment of inertia, and angular velocity are defined in the *PART INERTIA keyword. The mass of the pendulum plate must be 1500 kg with a width and height of 2500 mm and 800 mm, respectively. In addition, the center of gravity of the pendulum plate must be 50 mm below the R point of the driver's seat. "R-Point" or seating reference point means a design point defined by the vehicle manufacturer for each seating position and established with respect to the three-dimensional reference system (see Figure 6). Moreover, the distance from the center of gravity of the pendulum plate to the rotation axis of the pendulum was taken as 3500 mm, as stated by the ECE R29 regulation (Figure 6).²⁵ According to these geometrical constraints, the mass moment of inertia and angular velocity satisfying the required crash energy of 45 kJ was calculated.

The required angular velocity of the pendulum for the *PART INERTIA definition can be calculated using equation (1) for a kinetic energy of 45 kJ

$$E = \frac{1}{2} I_{yy} \omega_y^2 \quad (1)$$

where I_{yy} and ω_y are the mass moment of inertia and angular velocity of the pendulum respectively. Note that in this study, the mass moment of inertia and

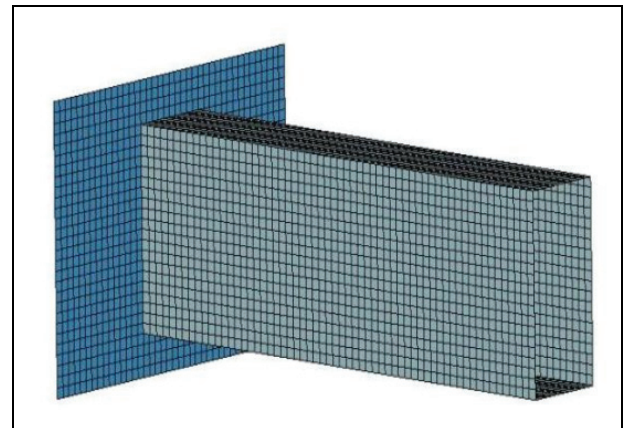


Figure 7. Finite element model of steel rectangular crash-box.²⁶

angular velocity is taken to be $I_{yy} = 18.4 \times 10^3 \text{ kg mm}^2$ and $\omega_y = 2.21 \text{ rad/s}$.

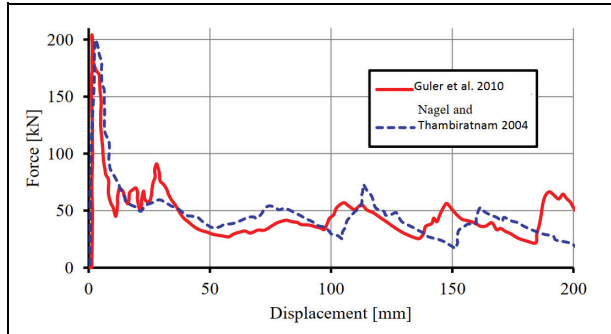
Energy absorber validation

The finite element model used for the bus body and the energy absorbers was validated based on the existing literature. The studies of Nagel and Thambiratnam²⁶ and Mamalis et al.²⁷ were used to validate the constructed finite element model. While the study of Nagel and Thambiratnam²⁶ was used for the validation of straight energy absorbers, the conical energy absorbers were validated using the study by Mamalis et al.²⁷

The straight energy absorber model was validated according to the same geometry, boundary conditions, and impact velocity as those of the study of Nagel and Thambiratnam,²⁶ the geometry is shown in Figure 7. Steel, with a yield stress of 304 MPa, was used as the material of the straight energy absorber, and its the true stress–true strain values are tabulated in Table 1. The

Table 1. True stress-strain values of steel.²⁶

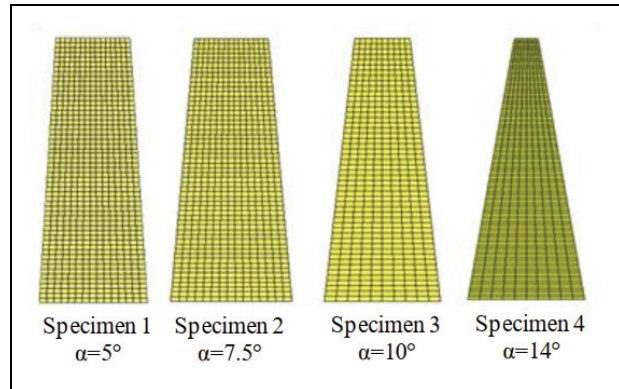
σ_t (MPa)	304.6	344.19	385.51	424.88	450.39	470.28
ϵ_p	0	0.0244	0.0485	0.0951	0.1384	0.191

**Figure 8.** Force-displacement graph of numerical model of the crashbox shown in Figure 7.^{25,26}

length of the model is 300 mm and the wall thickness is 1.5 mm. The section measurements are 100 mm×50 mm, as mentioned in Nagel and Thambiratnam.²⁶ The plate on which the crushboxes are fixed at the rear is rigid. The rigid wall used in the crash weighted 90 kg with a speed of 15 m/s. The effect of the strain rate effect on the steel material was considered in the finite element model by using the Cowper-Symonds equation, given as follows

$$\dot{\epsilon}_p = D \left(\frac{\sigma'_0}{\sigma_0} - 1 \right)^q \quad (\text{for } \sigma'_0 \geq \sigma_0) \quad (2)$$

Here, $\dot{\epsilon}_p$ is the strain rate, σ'_0 is the dynamic current stress, σ_0 is static current stress, and D and q are the strain rate parameters. D and q in equation (2) are 6.844 ms⁻¹ and 3.91, respectively. These values are obtained for dynamic crushing of steel pipes and have been obtained from previous studies.^{28–31} The force-displacement graph of the numerical model is shown in Figure 8, in which the maximum and average crushing forces are 204 and 48 kN, respectively. The values obtained by Nagel and Thambiratnam²⁶ were 200 and 45.5 kN for maximum and average crushing forces,

**Figure 9.** Geometries of conical energy absorbers modeled in Mamalis et al.²⁷

respectively. The results obtained in the numerical model fit well with those in Nagel and Thambiratnam.²⁶ Moreover, the model in Nagel and Thambiratnam²⁶ absorbed 9.1 kJ while the model in Güler et al.²⁵ absorbed 9.6 kJ at a deformation length of 200 mm.

The finite element model for conical energy absorbers was verified using the results of the study by Mamalis et al.²⁷ The model used in the current study is a conical model with a rectangular cross section and length of 127 mm. Semi-taper angles were selected as 5, 7.5, 10, and 14 degrees. The element model of these four geometries is shown in Figure 9. In addition, Table 2 lists the geometric details of the model used in the verification study. Table 3 compares the current results obtained with those of Nagel and Thambiratnam²⁶ and Mamalis et al.²⁷ and shows that the results are similar.

Experimental setup and validation

To determine the accuracy of the numerical model, the base bus model, which was the model of our previous study,³² was hit with a pendulum in numerical analysis, and the images obtained from the analysis were compared with the test results. Collision tests were performed on a pendulum test device designed according to the ECE R29 regulation (see Figure 10). The test was recorded using a Fastec TroubleShooter HR fast camera capable of shooting 500 fps at 1280×1024 resolution. The numerical analysis results were validated

Table 2. Geometric details used in the verification.²⁷

	Specimen 1	Specimen 2	Specimen 3	Specimen 4
Base dimensions (mm)	34.5×35.6	35.7×36.4	26.5×27.5	11.7×11.6
Top dimensions (mm)	50.0×51.9	58.5×59.1	55.8×57.2	56.8×56.5
Height (mm)	127	127	127	127
Wall thickness (mm)	0.97	1.47	1.6	1.52
Semi-apical angle (°)	5°	7.5°	10°	14°
Number of shell elements	3300	3300	2000	4400
Impacter mass (kg)	60	60	60	60
Impact velocity (m/s)	6.05	9.1	9.25	8.7

Table 3. Comparison of the results of the finite element model with those of the previous studies.

		Semi-apical angle ($^{\circ}$)			
		5 $^{\circ}$	7.5 $^{\circ}$	10 $^{\circ}$	14 $^{\circ}$
Nagel and Thambiratnam ²⁶	Crush distance (mm)	87.97	88.30	84.30	98.56
	Total energy absorption (kJ)	1.08	2.42	2.40	2.29
Mamalis et al. ²⁷	Crush distance (mm)	89.50	83.50	89.00	90.50
	Total energy absorption (kJ)	1.04	2.67	2.50	2.07
Güler et al. ²⁵	Crush distance (mm)	88.57	84.36	80.64	95.20
	Total energy absorption (kJ)	1.08	2.45	2.52	2.24

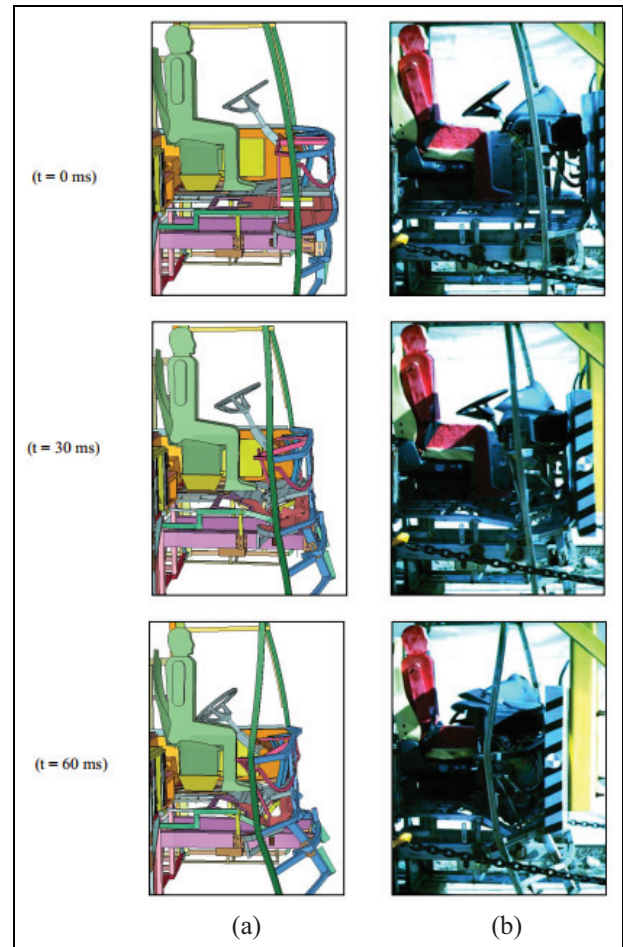
**Figure 10.** Crash test including pendulum and bus structure.

using camera images. Figure 11 provides the comparison of the numerical analysis results with the test results obtained through the fast camera. The comparisons show that the deformations in the bus body are similar to each other. Especially, when the behavior of the steering wheel is examined, the test and analysis results are similar. Moreover, when the crushing behaviors of the front profiles of the bus are examined, deformations of the longitudinal profiles carrying the driver's lower platform and the front profiles are similar.

The crushing behaviors of the profiles carrying the driver platform and the profiles extended along the direction of impact were similar. Some profiles in the analysis also experienced tearing. Figure 12 shows the rupture in the profiles with the driver platform. Furthermore, some profiles were found to undergo global buckling under impact in both numerical and test results.

Numerical results

The existing (baseline) bus body and the weaker regions of the body were first numerically analyzed. As

**Figure 11.** Comparison of progressive deformations: FEM and pendulum test.

expected, the baseline bus model did not meet ECE R29 requirements which require the steering wheel does not damage the mannequin after the test being conducted. The baseline bus body failed in the frontal crash test owing to the damage in the driver quarters.

The analysis and testing of the existing bus body resulted in the determination of weaker zones of the structure and these zones were then strengthened. The improvements include an increase in the thickness of the required profiles, strengthening the structure by adding a reinforced profile, and addition of energy absorber. Although it was not adequate, the

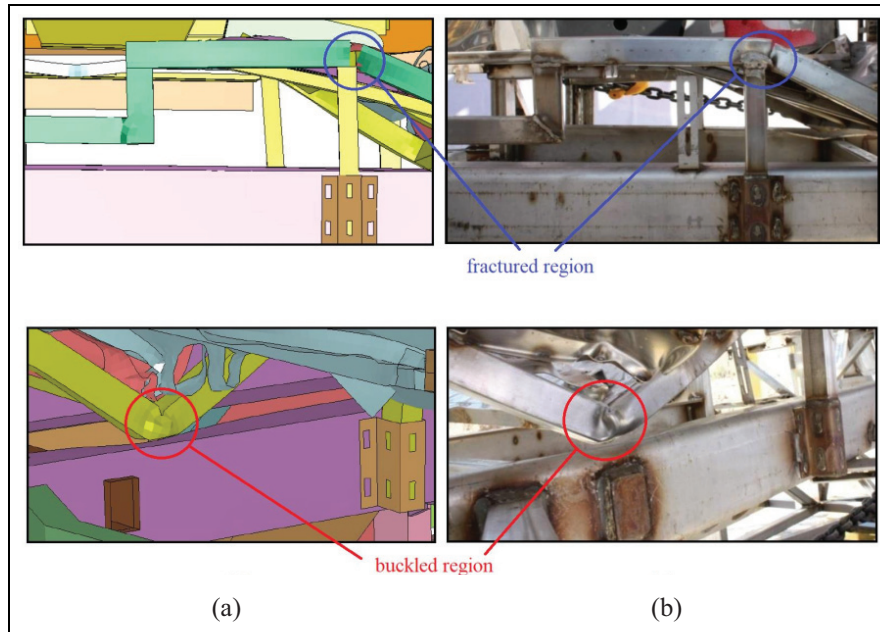


Figure 12. Comparison of the profiles carrying the driver subplatform; (a) FEM and (b) test.

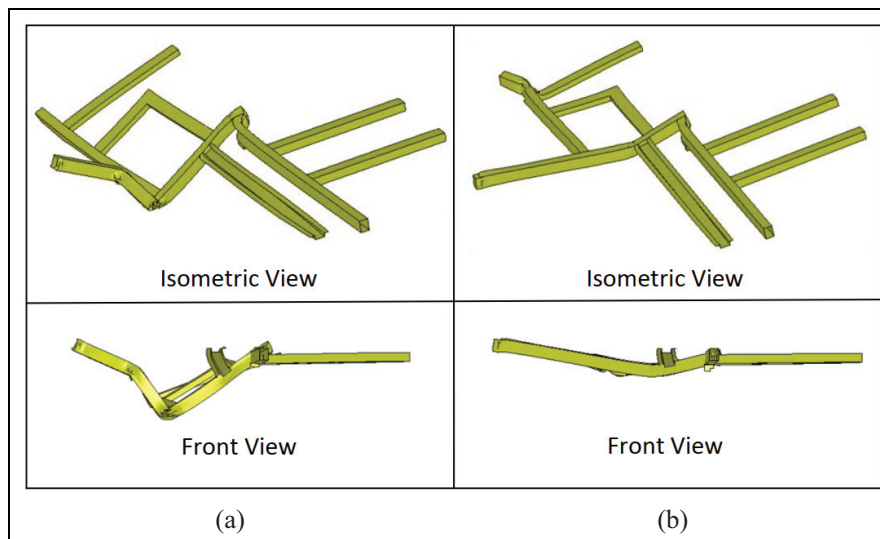


Figure 13. Crushing of the profiles carrying the six platforms of the driver: (a) before improvement and (b) after improvement.

strengthening of the weak profiles at the body has contributed positively to energy absorption and drive life. To improve the energy absorption without violating the driving compartment, an improved energy absorber was constructed in the reinforced body. Reinforced profiles and cage structure were built on the front of the vehicle so that the energy absorbers can be mounted and firmly supported from the rear. These reinforced profiles have been supported by scooping to ensure the robust construction required for energy absorbers. Figure 13 shows the change in the crushing behaviors of the profiles carrying the driver sub-platform after the crash analysis of the improved body.

After the crash, energy-absorbing geometries were designed to increase the driver survival space. These energy absorbers were collided with the numerical pendulum model independent of the bus body before being subjected to analysis by mounting on the bus body. The time-dependent crushing behaviors of energy absorbers are shown in Figure 14. The energy absorption characteristics of the energy absorbers analyzed independently of the bus body are shown in Table 4. The average crushing force (F_{mean}) was calculated at 80 mm. The crush force efficiency (CFE) as well as the SEA of the energy absorbers are also provided in Table 4. The definitions of CFE and SEA can be found in Acar et al.³³

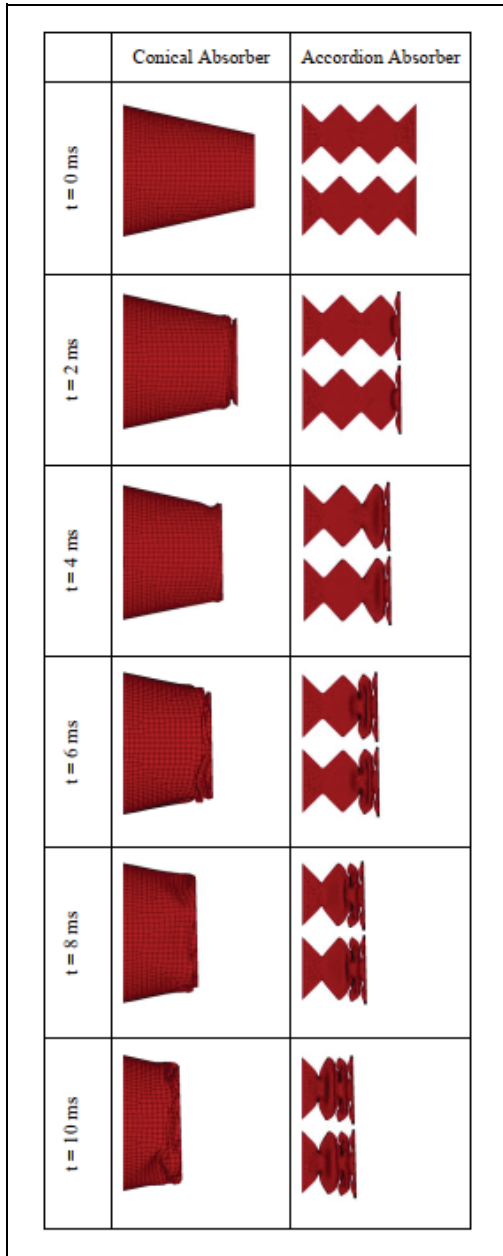


Figure 14. Time-dependent crushing behaviors of energy absorbers.

Energy absorbers have been added to the reinforced bus body in different geometries to increase energy absorption and protect the driving compartment. Two different alternative energy absorber designs were

added to the bus body and crash analyses were performed. One of these designs consisted of conical energy absorbers with a circular section, while the other consisted of an accordion geometry. The conical and accordion energy absorbers before and after the crash are shown in Figure 15.

According to analysis, the bus body with three conical energy absorbers was found to be better than the existing design (Case 1). The steering wheel drive or other parts were not attached to the driver’s compartment. However, as the distance between the steering wheel and mannequin is very short, sufficient safety is not provided. In the body including the accordion energy absorber, the steering wheel is kept away from the driver’s compartment and completely protected (Case 2). Figure 16 shows the existing body analysis, and comparison of the progressive deformations in Cases 1 and 2.

As shown in Figure 16, the current body did not satisfy the need to protect the driver compartment and failed to satisfy the ECE R29 requirements. Case 1, which includes the conical energy absorber, shows a critical situation due to preservation of the survival space; however, the steering wheel and mannequin are extremely close. In Case 2, which includes the accordion-shaped energy absorbers, the driving quarters were preserved and the ECE R29 requirements were satisfied (i.e. no intrusions to the survival space of the driver).

Case 2 showed the best performance among the three body analyses, and would be appropriate for examining the displacement of the steering wheel. Vertical and horizontal displacements of a point on the steering wheel were examined and compared for the three bodies (Figure 17(a) and Table 5). For Case 2, the steering wheel is more restricted both in the horizontal and vertical directions compared to those of the other cases. The variation of the vertical and horizontal displacements of the steering wheel during 120 ms impact time frame is provided in Figure 17(b). In addition to the steering wheel, three additional points are selected on the front body (see Figure 18), and the variations of the horizontal and vertical displacements of those points during 120 ms impact time frame are provided in Figures 19 and 20.

In the analyses, the energy was controlled and it was checked whether the energy was protected. In addition, this study examined how much of the total energy was converted. Figure 21 plots the initial kinetic energy, internal energy, hourglass energy, and sliding energy

Table 4. Results of pendulum analysis for energy absorbers.

Absorber	Absorbed energy (kJ)	Max crash force (F_{max}) (kN)	Mean crash force (F_{mean})* (kN)	CFE (%)	SEA (kJ/kg)
Conical (Case 1)	9.1	132.1	113.8	86	6.39
Accordion (Case 2)	11.7	215.4	146.3	68	1.57
Conical accordion	4.3	42.8	53.8	79	1.26

CFE: crush force efficiency; SEA: specific energy absorption.

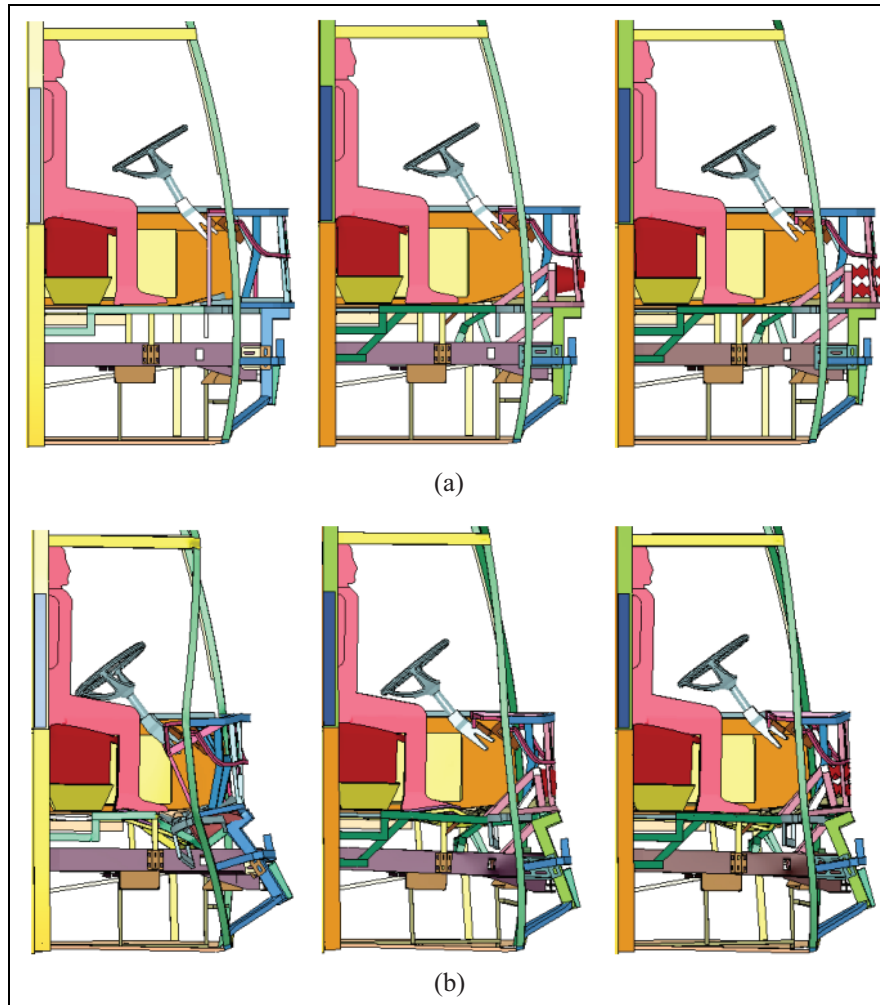


Figure 15. View of bus structures (a) before and (b) after impact.

curves. Approximately 43 kJ of the first kinetic energy of 45 kJ is converted to internal energy, and the remaining part of the kinetic energy was converted to sliding and hourglass energies. The stabilization requirement is provided to conform to the principle of conservation of the energy. Moreover the hourglass energy value fulfills this requirement because the hourglass energy is less than 10% of the internal energy. In addition to the steering wheel, three additional points are selected on the front body (see Figure 18), and the variation of the horizontal and vertical displacements of those points during 120 ms impact time frame is provided in Figures 19 and 20 (see Figure 17(b)).

An energy-absorbing reinforcement was made to increase the energy absorption capacity of the bus body. The contribution of the added energy absorbers to energy absorption should be examined. The determination of the amount of the internal energy absorbed by energy absorbers is significant for determining the success of energy absorbers. The contributions of the different energy absorbers in comparison with the total energy absorption (Case 1 and Case 2) are shown in Figure 22. Circular cross-sectional cone energy

absorbers provide 7.6 kJ energy absorption, while accordion-shaped absorbers absorb 8.9 kJ energy (Table 5).

Among the two tested energy-absorbing systems, the bus body using the accordion-type energy absorbers satisfied ECE R29 requirements. Apart from this energy absorber, a significant portion of the energy absorption was provided by the other profiles forming the bus body. Figure 23 shows contribution of bus components to energy absorption. The accordion-shaped energy absorbers provide maximum energy absorption, and front cage profiles, under-drive profiles, under-drive panels, and front cage support brackets also provide significant energy absorption.

Although the most important parameter in an energy absorbing structure is the absorbed energy value, it should not be considered alone. When examining the energy absorption characteristic, the maximum crushing forces occurring in the structure during crash should also be considered. When the crushing force is very high, the impact force will be transmitted to the driver and passenger compartment. Therefore, the forces generated during the crash must also be

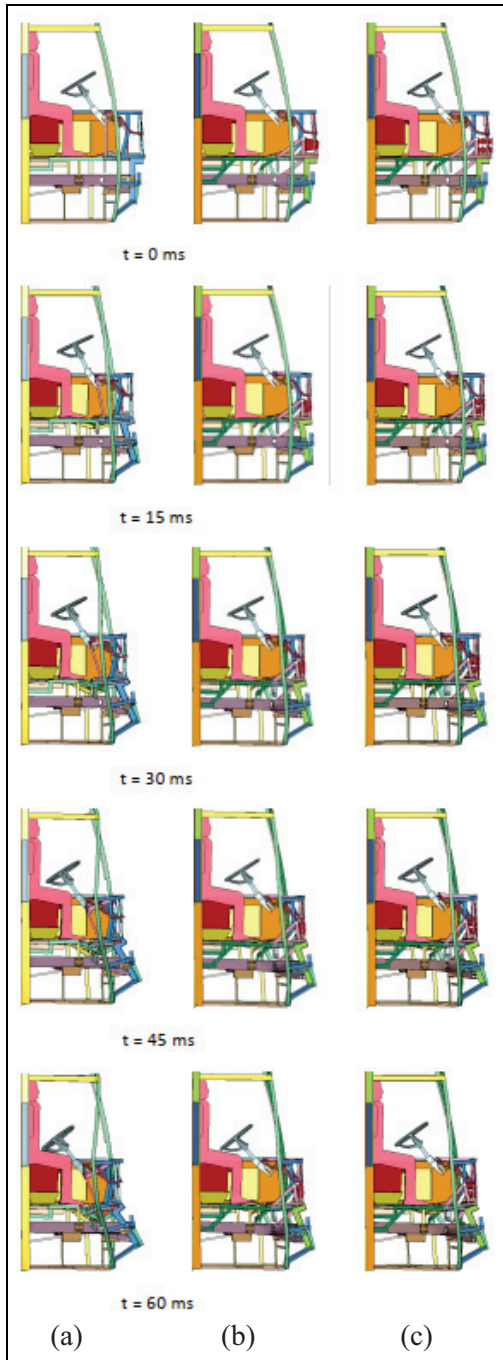


Figure 16. Progressive deformations of three bus structures at different time intervals (a) baseline, (b) Case 1, and (c) Case 2.

Table 5. Absorbed energy via energy absorbers and displacement of the selected node on the steering wheel.

	Absorbed energy via energy absorbers (kJ)	Displacement of the steering wheel	
		Δ_x (mm)	Δ_z (mm)
Baseline	—	233	107
Case 1 (conical absorbers)	2*7.6	2*130	2*146
Case 2 (accordion shaped absorbers)	2*8.9	2*112	2*78

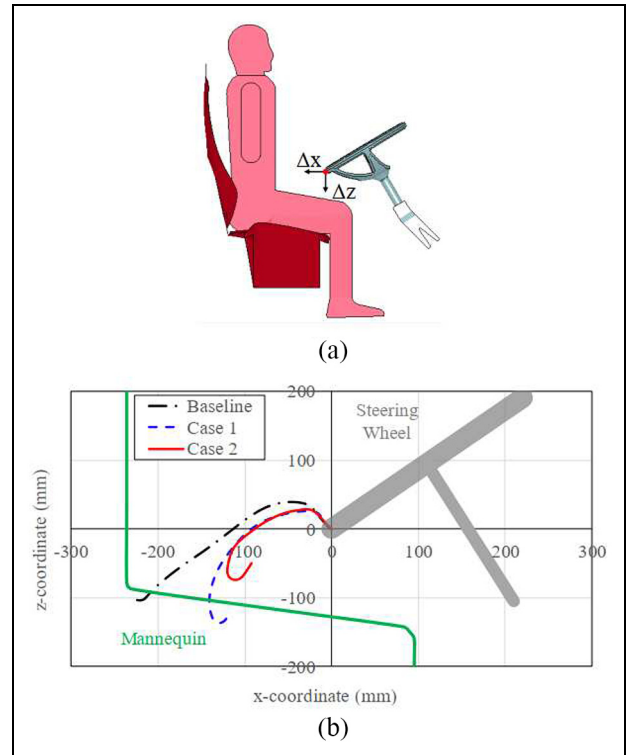


Figure 17. (a) Position of the steering wheel with respect to mannequin (Point I) and (b) variation of the displacement of point I during 120 ms impact time frame.

examined. Figure 24 shows force-time graphs for the existing bus body, Case 1, and Case 2. As expected, owing to the weakness of the existing baseline, very low force was produced compared to the other two models. In Cases 1 and 2, which respectively include the reinforced and additional energy-absorber, relatively higher force values are obtained. The comparison of Cases 1 and 2 showed that the accordion-type energy absorber in Case 2 has lower force values than that in Case 1 except between 0 and 20 ms. Therefore, the body including the accordion-shaped energy-absorber provides more efficient energy absorption than the body including the conical energy absorber in terms of energy absorption and crushing strength.

Conclusion

This study focused on passive safety for frontal crash situations in buses. The paper presented the results obtained from tests and simulations based on ECE R29 regulation for the frontal crash state. The finite element model was validated for both energy absorbers and for the bus at the baseline.

After the validation of the finite element model, the study aimed to increase the strength of the front of the bus body against crash. Therefore, the analysis and test results of the baseline body were used to identify the weaker regions of the body requiring reinforcement, and these regions were strengthened.

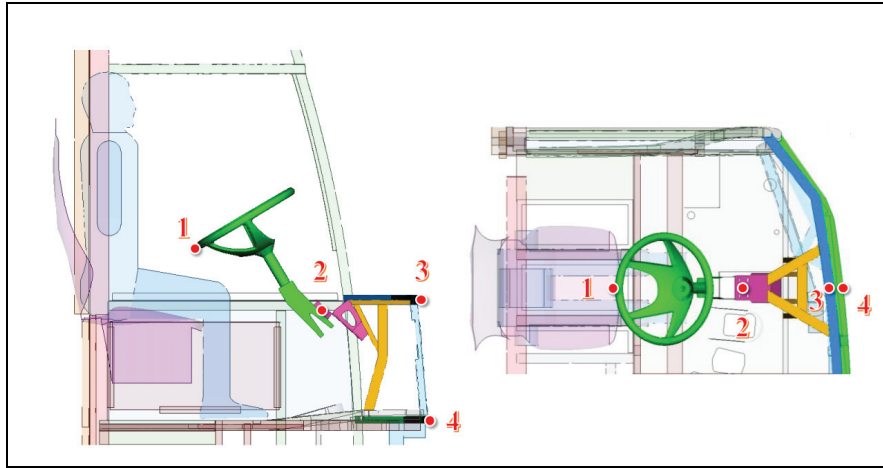


Figure 18. Points selected on the front body for the calculation of displacements.

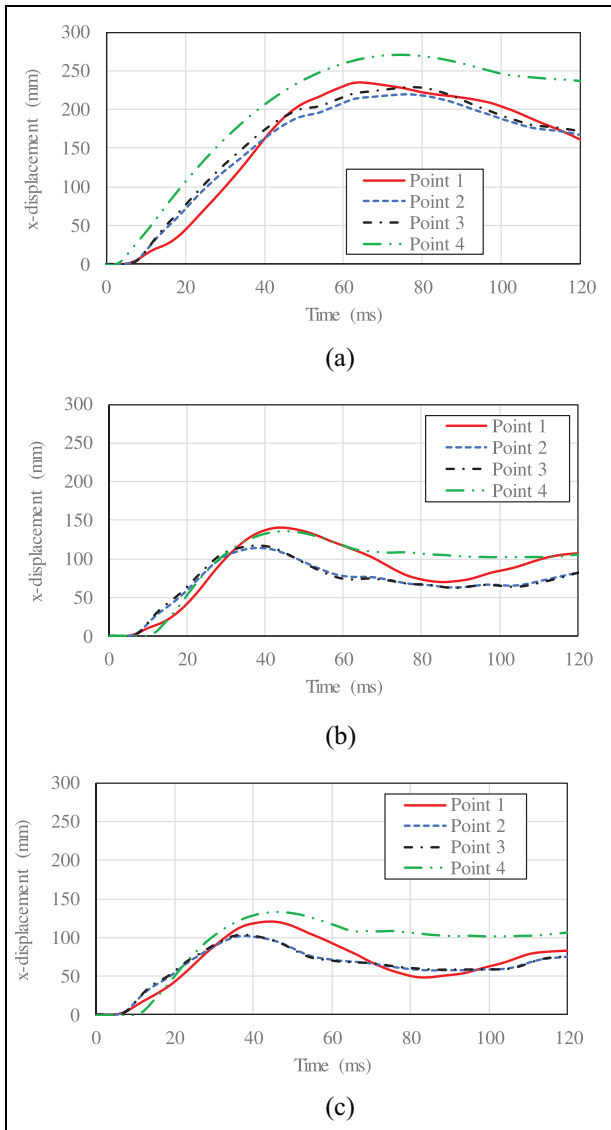


Figure 19. Variation of the horizontal displacements of the selected points during 120 ms impact time frame.

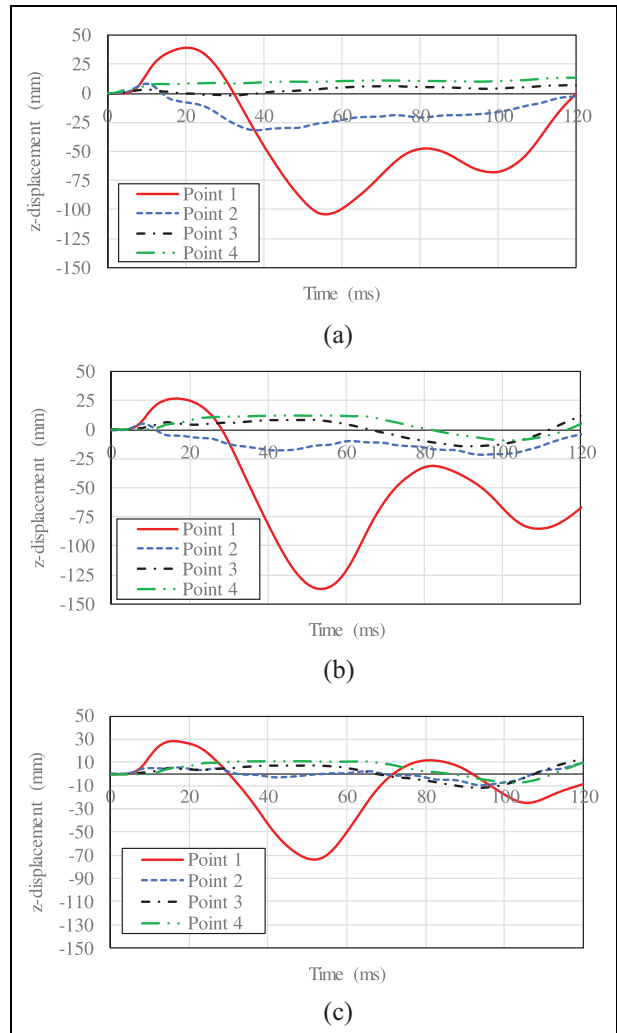


Figure 20. Variation of the vertical displacements of the selected points during 120 ms impact time frame: (a) baseline, (b) Case 1, and (c) Case 2.

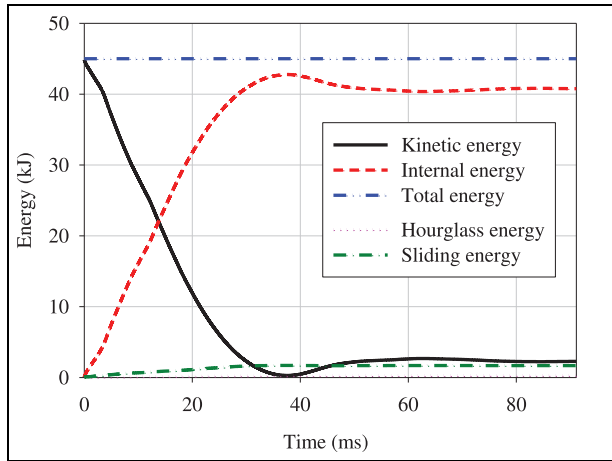


Figure 21. Energy-time graph of the crash analysis.

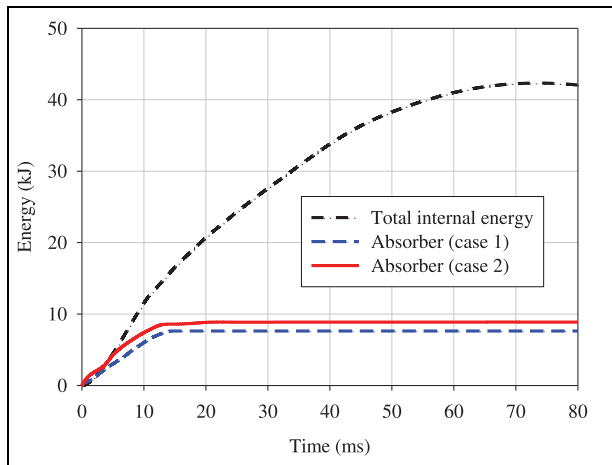


Figure 22. Energy absorption behavior of Cases 1 and 2.

While determining the crash performances of the bus, the SEA and CFE values obtained from the analysis for different crash boxes were considered:

- Conical absorber with the best CFE performance also shows the best SEA performance. The CFE and SEA values were computed as 86% and 6.39 kJ/kg, respectively.
- However, the accordion absorber that absorbed the maximum energy has the highest value for maximum crash force. The best value for maximum crash force was obtained by conical accordion model, that is 42.8 kN, which is five times smaller than the accordion design with the worst maximum crash force.
- According to the analysis, the bus body with the accordion-shaped energy absorber was found to outperform the existing and other designs. This model absorbed 8.9 kJ of energy, and the movement of the steering wheel is more restricted both

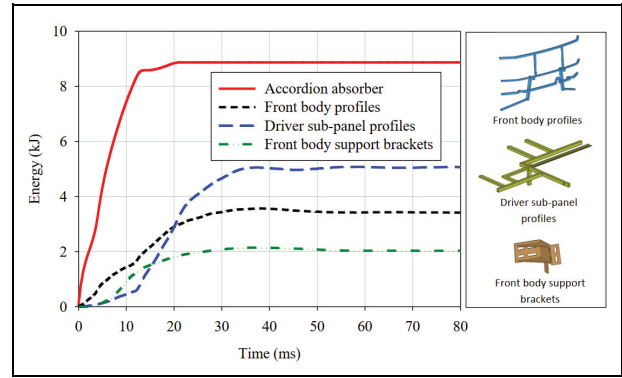


Figure 23. Energy absorption behavior of components.

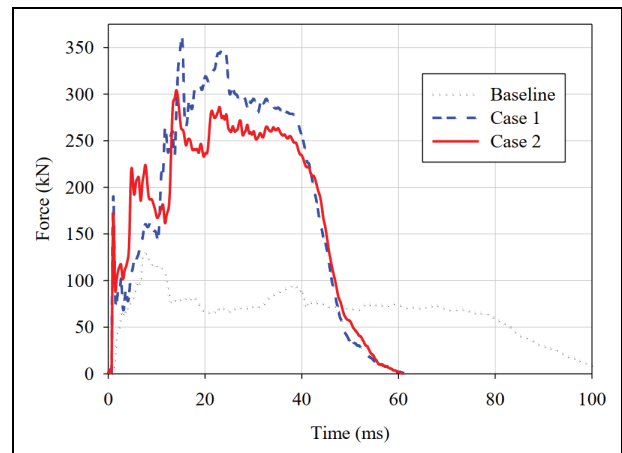


Figure 24. Reaction force behavior of three bus structures: baseline, Case 1, and Case 2.

in the horizontal and vertical direction than other models.

- In the analysis of bus systems, the bus body using the accordion-type energy absorbers satisfied ECE R29 requirements, although the bus at the baseline did not satisfy the requirements.

The energy absorber at the front of the body was reinforced to increase energy absorption. As a result of energy-absorber reinforcement, the bus body becomes more durable.

Acknowledgements

The authors would like to thank Dr. Ulrich Stelzmann of CADFEM and Bertan Bayram of TEMSA for their contributions to this study.

Declaration of conflicting interests

The author(s) declared no potential conflicts of interest with respect to the research, authorship, and/or publication of this article.

Funding

The author(s) disclosed receipt of the following financial support for the research, authorship, and/or publication of this article: This study was funded by the Turkish Ministry of Industry and Trade and TEMSA AR-GE VE TEKNOLOJİ A.Ş. within the scope of the SAN-TEZ project 00236.STZ.2008-1.

ORCID iDs

Mehmet Ali Güler  <https://orcid.org/0000-0002-1159-556X>

Erdem Acar  <https://orcid.org/0000-0002-3661-5563>

References

- Mayrhofer E and Steffan H. *Enhanced coach and bus occupant safety*. UNECE Informal Document No. GRSG-86-4, 19–23 April 2004. Geneva: United Nations Economic Commission for Europe (UNECE).
- Evaluation of occupant protection in buses (Prepared for: Road safety and motor vehicle regulation (ASFBE), 2002, <https://www.tc.gc.ca/media/documents/roadsafety/tp14006e.pdf>
- National highway traffic safety administration (NHTSA). Fatality Analysis Reporting System (FARS), <http://www-fars.nhtsa.dot.gov/Vehicles/VehiclesBuses.aspx> (accessed 22 May 2020).
- Raich H and DaimlerChrysler AG. Safety analysis of the new actros megaspaces cabin according to ECE-R29/02. In: *Proceedings of the 4th European LS-DYNA users conference*, pp.22–23, <https://www.dynamore.de/de/download/papers/konferenz03/crash-automotive-applications/safety-analysis-of-the-new-actros-megaspaces-cabin>
- Matolcsy M. Technical questions of bus safety bumpers. In: *Proceedings: International technical conference on the enhanced safety of vehicles*, Paper No. 05-0161, vol. 2005, pp. 9p–9p. National Highway Traffic Safety Administration.
- Marzbanrad J, Alijanpour M and Kiasat MS. Design and analysis of an automotive bumper beam in low-speed frontal crashes. *Thin Wall Struct* 2009; 47: 902–911.
- Tech TW, Iturrioz I and Morsch IB. Study of a frontal bus impact against a rigid wall. *WIT Trans Eng Sci* 2005; 49: 1–11.
- De Coo P, Hazelebach R, Van Oorschot E, et al. Improved safety for drivers and couriers of coaches. In: *Proceedings of the 17th international technical conference on the enhanced safety of vehicles*, Amsterdam, 4–7 June 2001. *The Hague: TNO Publications*.
- Griškevičius P and Žiliukas A. The crash energy absorption of the vehicles front structures. *Transport* 2003; 18: 97–101.
- Öztürk İ and Kaya N. Crash analysis of vehicle front bumper and its optimization. *Uludağ Univ J Fac Eng* 2008; 13: 119–127.
- Kokkula S, Hopperstad OS, Lademo OG, et al. Offset impact behaviour of bumper beam-longitudinal systems: numerical simulations. *Int J Crashworthiness* 2006; 11: 317–336.
- Kwasniewski L, Bojanowski C, Siervogel J, et al. Crash and safety assessment program for paratransit buses. *Int J Impact Eng* 2009; 36: 235–242.
- Güler MA, Elitok K, Bayram B, et al. The influence of seat structure and passenger weight on the rollover crashworthiness of an intercity coach. *Int J Crashworthiness* 2007; 12: 567–580.
- Güler MA, Atahan AO and Bayram B. Crashworthiness evaluation of an intercity coach against rollover accidents. *Int J Heavy Veh Syst* 2011; 18: 64–82.
- Demirci E and Yıldız AR. An investigation of the crash performance of magnesium, aluminum and advanced high strength steels and different cross-sections for vehicle thin-walled energy absorbers. *Mater Test* 2018; 60: 661–668.
- Tanlak N, Sonmez FO and Senaltun M. Shape optimization of bumper beams under high-velocity impact loads. *Eng Struct* 2015; 95: 49–60.
- Xiao Z, Fang J, Sun G, et al. Crashworthiness design for functionally graded foam-filled bumper beam. *Adv Eng Softw* 2015; 85: 81–95.
- Belingardi G, Beyene AT and Koricho EG. Geometrical optimization of bumper beam profile made of pultruded composite by numerical simulation. *Compos Struct* 2013; 102: 217–225.
- Kiani M and Yıldız AR. A comparative study of non-traditional methods for vehicle crashworthiness and NVH optimization. *Arch Comput Meth Eng* 2016; 23: 723–734.
- Karagöz S and Yıldız AR. A comparison of recent meta-heuristic algorithms for crashworthiness optimisation of vehicle thin-walled tubes considering sheet metal forming effects. *Int J Veh Des* 2017; 73: 179–188.
- United Nations Economic Commission for Europe (UNECE). *Uniform provisions concerning the approval of vehicles with regard to the protection of the occupants of the cab of a commercial vehicle*. Technical Report ECE R-29, 1998. Geneva: United Nations Economic Commission for Europe (UNECE).
- ANSA. *ANSA user guide*. Thessaloniki: ANSA, 2019.
- Livermore Software Technology Corporation. *LS-DYNA keyword user's manual*. Livermore, CA: Livermore Software Technology Corporation, 2017, p.970.
- Dassault Systemes of America Corporation. *CATIA*. Woodland Hills, CA: Dassault Systemes of America Corporation, 2017.
- Güler MA, Cerit ME, Bayram B, et al. The effect of geometrical parameters on the energy absorption characteristics of thin-walled structures under axial impact loading. *Int J Crashworthiness* 2010; 15: 377–390.
- Nagel G and Thambiratnam D. Dynamic simulation and energy absorption of tapered tubes under impact loading. *Int J Crashworthiness* 2004; 9: 389–399.
- Mamalis A, Manolacos D, Ioannidis M, et al. Finite element simulation of the axial collapse of thin-wall square frusta. *Int J Crashworthiness* 2001; 6: 155–164.
- Abramowicz W and Jones N. Dynamic axial crushing of square tubes. *Int J Impact Eng* 1984; 2: 179–208.
- Abramowicz W and Jones N. Dynamic progressive buckling of circular and square tubes. *Int J Impact Eng* 1986; 4: 243–270.
- Reid SR, Reddy TY and Gray MD. Static and dynamic axial crushing of foam-filled sheet metal tubes. *Int J Mech Sci* 1986; 28: 295–322.
- Reid SR and Reddy TY. Static and dynamic crushing of tapered sheet metal tubes of rectangular cross-section. *Int J Mech Sci* 1986; 28: 623–637.

32. Cerit ME, Güler MA, Bayram B, et al. Improvement of the energy absorption capacity of an intercity coach for frontal crash accidents. In: *Proceedings of the 11th international LS-DYNA users conference*, <https://www.dyna look.com/conferences/international-conf-2010/CrashSafety-3.pdf>
33. Acar E, Güler MA, Gerçeker B, et al. Multi-objective crashworthiness optimization of tapered thin-walled tubes with axisymmetric indentations. *Thin Wall Struct* 2011; 49: 94–105.